Solar Resource Assessment Using GHI Measurements at a Site in Northeast India

A. Maisanam, B. Podder, K. K. Sharma and Agnimitra Biswas

Abstract The paper presents a detailed analysis of global solar radiation received during the year 2016 at a site in Northeast India. The variation of the solar resource is estimated by performing a statistical analysis on the monthly, daily and hourly basis. The frequency distribution of the hourly global solar radiation for each month is also presented. Using similar statistical analysis, the clearness index of the site is also estimated. The results show a high intensity of global horizontal radiation. During the study period, the average daily global solar radiation at Silchar is found to be 4231.5 W/m^2. The frequency distribution study shows that about 50% of times the hourly received global solar energy is more than 400 W/m^2. With an average clearness index of 0.54 and with 84% of partly clear and clear days during the year, the region gives an opportunity to trap the solar energy by application of solar conversion devices.

Keywords Global horizontal irradiation · Clearness index · Frequency distribution

1 Introduction

In the Paris climate conference (COP21), India has pledged to generate 40% of its ever-growing energy demands through renewable energy sources by 2030 [1]. The national program such as Jawaharlal Nehru National Solar Mission (JNNSM) with the commitment of generating 175 GW solar power by 2022 shows the attempt to combat global warming and climate change as well as improve the energy scenario of the rural region. The Northeast region of India is lagging behind the other regions in terms of per capita consumption. According to the Central Energy Authority report (CAE) 2016*, the average per capita consumption in northeast region is 300 units per person per year which is well below the national average of 900 units per person per year. The disparity in terms of development and low access to electricity is evident from the above data. Slow development in this region is also due to its difficult terrain. In such a scenario, decentralized solar energy systems can play a

A. Maisanam (✉) · B. Podder · K. K. Sharma · A. Biswas
Department of Mechanical Engineering, NIT Silchar, Silchar 788010, India
e-mail: hianil09@gmail.com

B. B. Biswal et al. (eds.), *Advances in Mechanical Engineering*, Lecture Notes in Mechanical Engineering, https://doi.org/10.1007/978-981-15-0124-1_111

vital role in improving energy access to this region. In order to design an optimum solar energy system, a thorough study of its solar resource is prerequisite. The solar potential assessment studies can be found in many literature where the study mainly focused on the data prediction of solar radiation data using empirical relations [2, 3]. The prospect of setting up solar conversion technologies was analysed in the various districts of Karnataka using remote sensing techniques, GIS and meteorological data from IMD Pune. From the study it was concluded that the coastal regions receive sufficient solar irradiation to set up solar conversion systems [4, 5]. With the help of Artificial Neural Network (ANN), the solar potential of Himachal Pradesh was analysed and it was reported that the state receives an annual global solar radiation between 3.59 and 5.38kWh/m^2/day, which indicates a potential scope for solar power generation [6]. In Ref. [7] the solar potential of coastal area of India is estimated. A statistical comparison of solar potential at two sites in Cyprus with different climatic condition has been studied [8, 9].

The present study estimates the monthly averaged daily and hourly variation of radiation intensities along with frequency distribution, which is important for design of a system. Variation is shown by computing the mean daily and hourly radiation for each month. It is also important to understand the sky condition of the region to understand the seasonal variation in the solar energy output. In order to categorise the sky condition, clearness index is also computed. The study is based on the GHI measured at the Regional Test Centre-cum-Technological Back-up Unit for Solar Thermal Devices (Solar RTC), NIT Silchar.

2 Details of Study Location and GHI Measurements

The study is performed at the Cachar district of Assam in Northeast India. It is located at Latitude: 24.8333° N, Longitude: 92.7789° E and its elevation is 25 m above sea level. According to the census 2011, the population of 17.37 lakh settled in 3786 sq. km area. It has a tropical climate and monsoon begins from June and lasts till September. The average annual temperature is 24.9 °C.

Study shows that India receives high solar insolation and the average solar radiation received ranges from 4–7 kWh/day [2, 10]. But due infrastructural gap in northeast region, studies using the real time data are not much reported. Therefore, in this study, the GHI data for the site is measured at the Solar RTC using pyranometer. At first, the Pyranometer is placed at a horizontal surface on the roof of the production engineering departmental building of NIT Silchar as shown in Fig. 1. The placement of the instrument is done in open space to avoid any shading. It collects the global horizontal radiation which is the combination of beam and diffuse radiation. In order to collect the diffuse radiation, a shading ring is fixed to the instrument which blocks the path of beam radiation. The measuring instrument is connected to a data logger from where data is downloaded and stored to a personal computer from time to time. The Datalogger takes the data at an interval of 1 min.

Fig. 1 Data measurement set up in the roof of production engineering departmental building of NIT Silchar

3 Uncertainty Analysis

While determining any measured data from various instruments, the knowledge of uncertainty associated with it is very much essential. The uncertainty in measurement usually depicts the ranges of values, in which the measured or true value lies within a certain stated probability. Uncertainties can be classified as Type A and Type B categories. The uncertainty evaluated in terms of the standard deviation of repeated measurements under similar conditions is known as Type A uncertainty and Type B

uncertainty is evaluated on the basis of the uncertainty of the values obtained from the calibration certificates of the equipment. In the present work, a Pyranometer is used for the measurement of solar irradiation and the methodology to obtain the uncertainties associated with it is described below:

Type A uncertainty:

Let G1, G2, G3… Gn be the 'n' number of solar irradiation considered for measuring the uncertainty of solar irradiation.

The average value of all the solar irradiation is evaluated as:

$$\overline{X} = \frac{1}{n}\sum_{i=1}^{n} G_i \tag{1}$$

Deviation of the measured values from the mean values can be obtained as:

Standard deviation is calculated as

$$d_1 = (G_1 - \overline{X})^2, d_2 = (G_2 - \overline{X})^2, d_3 = (G_3 - \overline{X})^2 \ldots$$
$$d_n = (G_n - \overline{X})^2$$

$$\sigma = \sqrt{\frac{1}{n-1}\sum_{i=1}^{n}\left(G_i - \overline{X}\right)^2} \tag{2}$$

Therefore, Type A uncertainty is given as

$$u_A = \frac{\sigma}{\sqrt{n}} \tag{3}$$

Type B uncertainty:

The standard deviation is given by, where is the expanded uncertainty of the Pyranometer at 95% confidence level with a coverage factor = 1.96.

Hence, Type B uncertainty is calculated as

$$u_B = \sqrt{(\sigma')^2} \tag{4}$$

Therefore, the combined uncertainty can be calculated as:

$$u_c = \sqrt{(u_A)^2 + (u_B)^2} \tag{5}$$

Expanded uncertainty is given by:

$$u_E = k \times u_c \tag{6}$$

The pyranometer used in the present work is calibrated at 95% confidence level with an expanded uncertainty of ± 0.0354 W/m^2. Therefore, using Eqs. (1)–(6), the uncertainty measurement of solar irradiation is found to be ± 0.90 W/m^2.

4 Result and Discussion

4.1 Variation of Solar Radiation

Solar radiation mainly comprises of the beam (received at the earth's surface without change of direction) and diffuse radiation (after being subjected to scattering in the atmosphere) and the summation is known as the global solar radiation. Figure 2 shows the monthly variation of various components of the global radiation and a comparison is done by including the extra-terrestrial radiation as well.

The highest monthly average daily global radiation is found to be 5.45 kWh/m^2 in the month of March. It can be observed from Fig. 2 that the solar output potential shows a decreasing trend from April. This decrease is due to the onset of monsoon season. The solar output potential again increases from the month of September and again there is decrease during the month of November and December as the sunshine hour decreases due to onset of winter season. During the year 2016, the monthly average daily accumulated global solar radiation is found to be 4231.5 W/m^2. The minimum monthly averaged daily accumulate solar energy occurs in the month of December with 3159.3 W/m^2. Table 1 provides the result of statistical analysis of hourly global radiation of an average day of each month which was performed in Microsoft excel. The results show that the maximum radiation intensity occurs in the month of March and October. The maximum mean is observed in the month of March with 427 W/m^2 and minimum mean value is 316 W/m^2, which is observed in the month of December. The median for most of the month is above 350 W/m^2 with only exception of two months. A lower coefficient of variance (CV) is desirable for giving more optimized design of solar devices. Although in case of this region the value of CV is observed on a higher side, with some over sizing the problem of

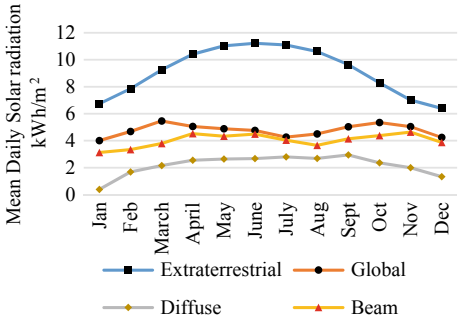

Fig. 2 Comparison of components of solar radiation with extra-terrestrial radiation

Table 1 Monthly statistical analysis of hourly global radiation at Silchar

Month	Min	Max	Q1	Median	Q3	Mean	SD	C.V.	Skewness	Kurtosis	SEM
Jan	106	545	209	354	476	337	159	0.47	– 0.175	– 1.568	52.84
Feb	146	589	249	413	542	386	162	0.42	– 0.256	– 1.659	53.90
March	73	684	263	462	618	427	203	0.48	– 0.256	– 1.279	64.24
April	87	659	252	390	568	386	186	0.48	– 0.192	– 1.243	56.15
May	91	601	263	429	545	393	168	0.43	– 0.593	– 0.912	50.74
June	121	561	251	386	521	373	154	0.41	– 0.371	– 1.217	46.48
July	96	542	238	341	484	342	151	0.44	– 0.249	– 1.313	45.62
Aug	86	577	218	361	532	360	182	0.50	– 0.211	– 1.606	54.76
Sept	85	650	264	450	559	408	182	0.45	– 0.298	– 1.194	57.71
Oct	71	684	237	448	630	423	216	0.51	– 0.275	– 1.582	68.21
Nov	88	662	209	396	580	392	203	0.52	– 0.166	– 1.653	64.07
Dec	86	522	182	329	455	316	154	0.49	– 0.155	– 1.658	51.45

higher CV can be mitigated. Skewness and Kurtosis value is generally used to define the type of frequency distribution.

4.2 Hourly Variation of Solar Radiation

The monthly averaged hourly variation of global solar radiation for each month is shown in the Fig. 3. For most of the month, extraction of solar energy will be better during 09:00–16:00 h as the radiation intensities are higher than 200 W/m^2. The maximum radiation intensity is available during 11:00–14:00 h for each month averaging approximately 600 W/m^2. To know the total amount of solar energy received during an average day of each month, a cumulative mean hourly global solar radiation is computed and is represented in Fig. 4. The Fig. 4 shows that the energy accumulated in an average day for the month of March to November is above 4000 W/m^2 and in the remaining months the accumulated energy is between 3000 and 4000 W/m^2. The reason for less accumulation of energy is due to the less sunshine hour available as the region experience its peak winter.

In Table 2, the maximum hourly global solar radiation received during the whole study period is represented. The peak radiation intensity is observed during the month of July with a value of 1028 W/m^2 between 11:00 and 12:00 h. As pointed out in Fig. 4, the peak hour of maximum radiation intensity extraction is from 11:00 to 14:00 h. In order to have more knowledge about the amount of energy accumulated during each time interval, the data measured were accumulated for each hour for all the months. Figure 5 represents the monthly accumulated hourly solar radiation, for the entire study period. It can be observed that the maximum energy of 21212.84 W/m^2

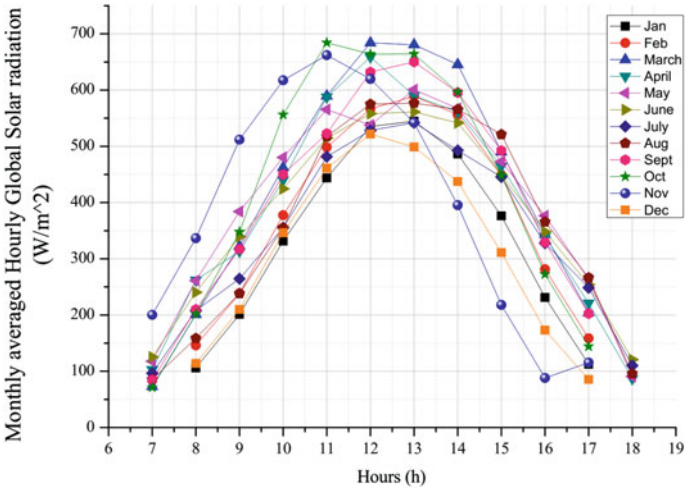

Fig. 3 Variation of monthly averaged hourly global radiation at Silchar

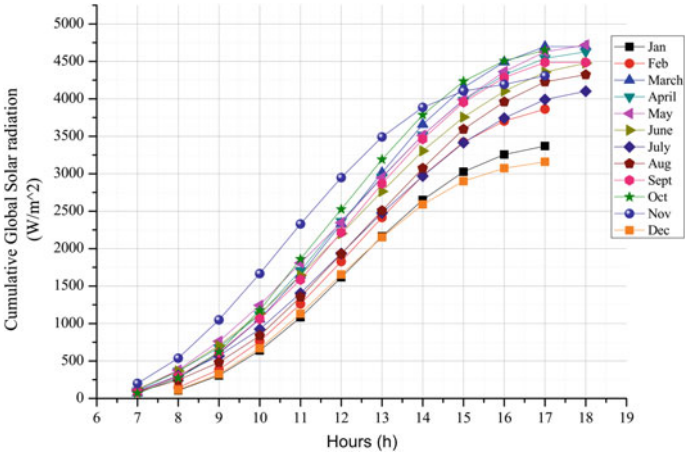

Fig. 4 Cumulative monthly averaged hourly global solar radiation at Silchar

is accumulated in the month of October between 10:00 to 11:00 h. But the average accumulation of energy is better from 11:00 to 13:00 h with a value of more than 17700 W/m^2 (Fig. 5).

4.3 Frequency Distribution of Hourly Global Solar Radiation

Table 3 shows the percentage frequency distribution of the hourly global radiation for each month. The knowledge of frequency distribution is highly required for setting up of solar energy systems. It can be observed that approximately 70% of the study period observed more than 200 W/m^2 global solar radiation intensities. October is most resourceful month as the radiation levels are above 500 W/m^2 for more than 40% of the time.

4.4 Clearness Index and Its Frequency Distribution

Clearness index (K_t) is the ratio of daily global radiation to the daily extraterrestrial radiation. It is used to categorize the sky condition. Sky condition is mainly categorized into cloudy days ($K_t < 0.35$), partly cloudy days ($0.35 \leq K_t < 0.65$), and clear days ($0.65 \leq K_t$), according to the value of clearness index [8, 9]. Table 4 represents the frequency distribution in % for each month for the entire study period. During the period of study, most of the days are having a good clearness index with a value of more than 0.50. But during the monsoon season (May–September), there is a drop in the clearness index due to cloudy condition of the sky. The average clearness index

Table 2 Hourly maximum global solar radiation (W/m^2) for each month at Silchar

Hour	Jan	Feb	March	April	May	June	July	Aug	Sept	Oct	Nov	Dec
06:00-07:00			73	168	192	197	134	127	129	81	74	
07:00–08:00	165	219	299	445	467	488	373	437	392	334	314	164
08:00–09:00	298	376	482	591	622	608	544	620	570	513	460	299
09:00–10:00	448	576	693	788	789	792	692	822	715	690	619	474
10:00–11:00	575	725	819	925	903	877	830	947	841	818	731	590
11:00–12:00	638	811	887	930	963	980	1028	989	974	838	786	647
12:00–13:00	668	819	866	926	942	933	933	965	1060	924	738	630
13:00–14:00	634	733	760	850	863	907	909	888	871	812	641	553
14:00–15:00	485	611	636	679	769	815	751	810	723	580	480	431
15:00–16:00	308	406	420	532	540	589	675	627	465	365	278	235
16:00–17:00	162	247	274	350	380	433	511	466	337	211	115	104
17:00–18:00				113	131	184	238	150				

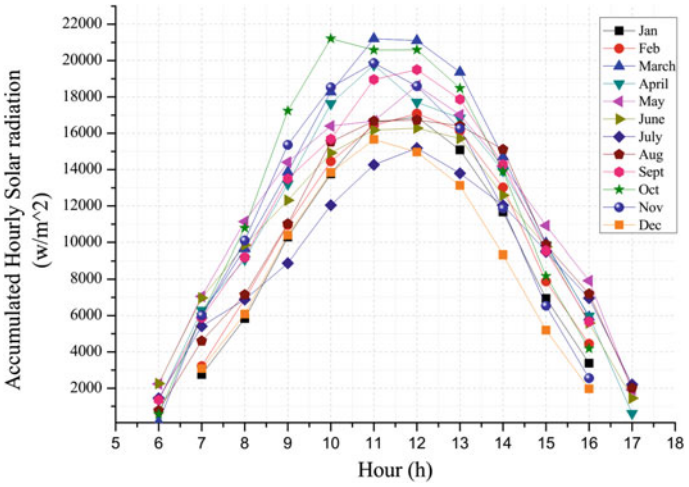

Fig. 5 Accumulated hourly global solar radiation

for each month is graphically represented in Fig. 6. It is observed that the average clearness index of the region is 0.54 for the year. The clearness index is acceptable as it is close to 0.65 but the average is lower due to very bad sky condition during the monsoon months which is evident from the Fig. 6.

5 Conclusion

This paper presents a detailed analysis of solar potential of Cachar District by measuring the solar data at the Solar RTC Silchar, NIT Silchar. The region of study has a good solar potential with a monthly average accumulated global radiation of 4231.5 W/m^2. The maximum global solar radiation is available during the months of March and October. The system installed in this type of region may require little oversizing as the statistical analysis shows that value of CV is little higher. The study of hourly variation of global solar energy shows that during 9:00–16:00 h most of the month receives more than 200 W/m^2 and the maximum solar energy is received during 11:00–13:00. In the entire study period, the accumulated daily solar radiation is more than 4000 W/m^2 except in the winter months (December, January and February) which also between 3000 and 4000 W/m^2. This indicates that the solar energy available for all the months are uniform which is desirable for system design. The maximum energy is accumulated during 10:00–11:00 h in the month of October and the accumulation of energy is maximum during 11:00–13:00 h for entire year. Frequency distribution study reveals that the almost 60% of the total study period received more than 300 W/m^2. This indicates a good opportunity for extraction of solar energy. 40–50% of the time the hourly global solar radiation is above 500 W/m^2.

Table 3 Frequency distribution in % of hourly global solar radiation (W/m^2) for each month at Silchar

Range	Jan	Feb	March	April	May	June	July	Aug	Sept	Oct	Nov	Dec
0–100	8.0	5.0	3.3	11.0	13.1	9.6	11.5	12.2	8.7	5.7	9.0	11.4
100–200	20.6	19.2	9.2	12.0	15.2	16.7	19.1	17.5	15.5	13.7	9.4	19.7
200–300	16.9	16.0	16.8	16.5	11.0	14.1	20.1	15.0	13.9	14.0	17.7	17.0
300–400	10.6	12.5	13.5	11.0	14.0	13.8	11.2	13.4	15.2	9.9	9.7	14.2
400–500	16.6	14.6	9.9	13.3	12.2	10.3	12.2	12.2	8.7	12.4	11.0	17.3
500–600	21.9	12.5	15.2	6.5	7.7	13.8	9.2	6.6	10.4	10.5	15.4	16.6
600–700	5.3	13.5	16.5	9.4	9.2	9.0	5.3	8.4	6.8	14.0	20.4	3.8
700–800	0.0	6.0	9.9	10.0	6.3	6.1	5.6	6.3	9.1	16.9	7.4	0.0
800–900	0.0	0.7	5.6	8.4	8.0	3.9	3.6	6.3	9.7	2.5	0.0	0.0
900–1000	0.0	0.0	0.0	1.9	3.3	2.6	2.0	2.2	1.6	0.3	0.0	0.0
1000–1100	0.0	0.0	0.0	0.0	0.0	0.0	0.3	0.0	0.3	0.0	0.0	0.0

Table 4 Frequency distribution in % of clearness index for each month at Silchar

K_t Range	Jan	Feb	Mar	Apr	May	Jun	Jul	Aug	Sept	Oct	Nov	Dec
0.00–0.20	0.0	0.0	3.2	13.3	3.2	6.7	0.0	6.5	3.3	0.0	0.0	0.0
0.20–0.25	3.2	0.0	0.0	0.0	6.5	3.3	17.2	6.5	10.0	0.0	0.0	0.0
0.25–0.30	0.0	3.4	0.0	3.3	3.2	3.3	13.8	9.7	6.7	3.2	3.3	0.0
0.30–0.35	0.0	3.4	0.0	6.7	12.9	10.0	13.8	9.7	3.3	0.0	0.0	3.3
0.35–0.40	6.5	3.4	0.0	6.7	19.4	16.7	6.9	9.7	3.3	0.0	0.0	3.3
0.40–0.45	3.2	6.9	3.2	10.0	12.9	20.0	10.3	3.2	3.3	3.2	3.3	6.7
0.45–0.50	0.0	6.9	9.7	3.3	9.7	13.3	17.2	16.1	6.7	6.5	0.0	6.7
0.50–0.55	12.9	10.3	22.6	10.0	3.2	10.0	17.2	19.4	10.0	9.7	0.0	13.3
0.55–0.60	12.9	10.3	12.9	13.3	6.5	3.3	0.0	16.1	10.0	0.0	3.3	10.0
0.60–0.65	25.8	6.9	12.9	20.0	12.9	10.0	3.4	3.2	10.0	19.4	6.7	13.3
0.65–0.70	16.1	20.7	12.9	10.0	5	3.3	0.0	0.0	20.0	16.1	6.7	20.0
0.70–0.75	19.4	24.1	19.4	3.3	3.2	0.0	0.0	0.0	13.3	29.0	33.3	20.0
0.75–0.80	0.0	3.4	3.2	0.0	0.0	0.0	0.0	0.0	0.0	12.9	23.3	3.3
0.80–0.85	0.0	0.0	0.0	0.0	0.0	0.0	0.0	0.0	0.0	0.0	16.7	0.0
0.85–0.90	0.0	0.0	0.0	0.0	0.0	0.0	0.0	0.0	0.0	0.0	3.3	0.0

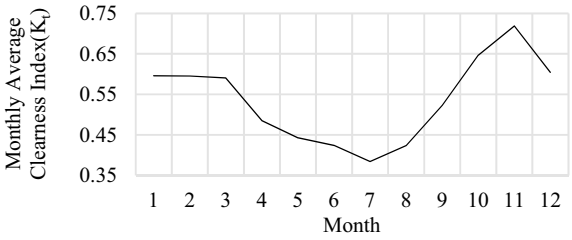

Fig. 6 Monthly variation of clearness index for an average day at Silchar

The sky condition of the region is categorized by computing clearness index. It has been observed that there is extremely low amount of cloudy days. The region is dominated with partly cloudy days but the clearness index during these days are close to 0.65 for most of the days. Almost 30% of the days during the studied period has been found to be clear day. Therefore, the region may require oversizing of system but with a good storage system, the oversizing can be reduced, thereby increasing the reliability of the plant.

Reference

1. Hairat, M.K., Ghosh,S.: 100 GW solar power in India by 2022-A critical review. Renew. Sustain. Energy Rev. **73**, 1041–1050 (2017).https://doi.org/10.1016/j.rser.2017.02.012
2. Mohanty, S., Patra, P.K., Sahoo, S.S., Mohanty, A.: Forecasting of solar energy with application for a growing economy like India: survey and implication. Renew. sustain. Energy Rev. **78**, 539–553 (2017). https://doi.org/10.1016/j.rser.2017.04.107
3. Ulfat, I., Javed, F., Abbasi, F.A., Kanwal, F., Usman, A., Jahangir, M., Ahmed, F.: Estimation of solar energy potential for Islamabad, Pakistan. In: Terragreen 2012: Clean Energy Solutions for Sustainable Environment (CESSE), vol. 18, pp. 1496–1500 (2012)
4. Ramachandra, T.V., Subramanian, D.K.: Potential and prospects of solar energy in Uttara Kannada, District of Karnataka State, India. Energy Sour. **19**, 945–988 (1997). https://doi.org/10.1080/00908319708908903
5. Ramachandra, T.V.: Solar energy potential assessment using GIS. Energy Edu. Sci. Technol. **18**, 101–114 (2006)
6. Yadav, A.K., Chandel, S.S.: Solar energy potential assessment of western Himalayan Indian state of Himachal Pradesh using J48 algorithm of WEKA in ANN based prediction model. Renew. Energy **75**, 675–693 (2015). https://doi.org/10.1016/j.renene.2014.10.046
7. Solanki, C., Nagababu, G., Kachhwaha, S.S.: Assessment of offshore solar energy along the coast of India. Energy Procedia. **138**, 530–535 (2017). https://doi.org/10.1016/j.egypro.2017.10.240
8. Kalogirou, S.A., Pashiardis, S., Pashiardi, A.: Statistical analysis and inter-comparison of the global solar radiation at two sites in cyprus. Renew. Energy **101**, 1102–1123 (2017). https://doi.org/10.1016/j.renene.2016.09.027
9. Pashiardis, S., Kalogirou, S.A., Pelengaris, A.: Statistical analysis for the characterization of solar energy utilization and inter-comparison of solar radiation at two sites in Cyprus. Appl. Energy **190**, 1138–1158 (2017). https://doi.org/10.1016/j.apenergy.2017.01.018
10. Sahoo, S.K.: Renewable and sustainable energy reviews solar photovoltaic energy progress in India: a review **59**, 927–939 (2016). https://doi.org/10.1016/j.rser.2016.01.049